

This document is the Accepted Manuscript version of a Published Work that appeared in final form in Analytical Chemistry, copyright © 2022 American Chemical Society after peer review and technical editing by the publisher. To access the final edited and published work see <https://doi.org/10.1021/acs.analchem.2c04589>

# Csm6-DNAzyme tandem assay for one-pot and sensitive analysis of lead pollution and bioaccumulation in mice

Hao Yang<sup>a</sup>, Feng Li<sup>b</sup>, Ting Xue<sup>a</sup>, Mohammad Rizwan Khan<sup>d</sup>, Xuhan Xia<sup>a</sup>, Rosa Busquets<sup>e</sup>, Hong Gao<sup>a,\*</sup>, Yi Dong<sup>a</sup>, Wenhui Zhou<sup>c</sup>, Ruijie Deng<sup>a,\*</sup>

<sup>a</sup> College of Biomass Science and Engineering, Sichuan University, Chengdu 610065, China

<sup>b</sup> Key Laboratory of Green Chemistry & Technology of Ministry of Education, College of Chemistry, Analytical & Testing Center, Sichuan University, Chengdu, Sichuan 610065, China

<sup>c</sup> Xiangya School of Pharmaceutical Sciences, Central South University, Changsha, Hunan 410013, China

<sup>d</sup> Department of Chemistry, College of Science, King Saud University, Riyadh, 11451, Saudi Arabia

<sup>e</sup> School of Life Sciences, Pharmacy and Chemistry, Kingston University London, Penrhyn Road, KT1 2EE, Kingston Upon Thames, United Kingdom

\*e-mail: Hong Gao, [gao523@hotmail.com](mailto:gao523@hotmail.com)

Ruijie Deng, [drj17@scu.edu.cn](mailto:drj17@scu.edu.cn)

## Abstract

Lead contamination in the environment tends to enter the food chain and further into the human body, causing serious health issues. Herein, we proposed a Csm6-DNAzyme tandem assay (termed cDNAzyme) using CRISPR/Cas III-A Csm6 and GR-5 DNAzyme, enabling one-pot and sensitive detection of lead contamination. We found that  $\text{Pb}^{2+}$ -activated GR-5 DNAzyme produced cleaved substrates that can serve as the activator of Csm6, and the Csm6-DNAzyme tandem improved the sensitivity for detecting  $\text{Pb}^{2+}$  by 6.1 times compared to the original GR-5 DNAzyme. Due to the high specificity of DNAzyme, the cDNAzyme assay can discriminate  $\text{Pb}^{2+}$  from other bivalent and trivalent interfering ions and allowed precise detection of  $\text{Pb}^{2+}$  in water and food samples. Particularly, the assay can achieve one-step, mix-and-read detection of  $\text{Pb}^{2+}$  at room temperature. We used the cDNAzyme assay to investigate the accumulation of lead in mice, and found that lead accumulated at higher levels in the colon and kidney compared to the liver, and most of the lead was excreted. The cDNAzyme assay is promising to serve as analytical tools for lead-associated environmental and biosafety issues

## Introduction

Lead(II) ion ( $\text{Pb}^{2+}$ ), which mainly resulted from the mining industry and the exhaust gas emission of automobiles, is one of the most widely distributed toxic metal contaminants in the ecological environment.<sup>1,2</sup> The USA Environmental Protection Agency (EPA) has identified it as a probable human carcinogen<sup>3</sup> and strictly limits the safe lead levels in drinking water to be 15 ppb (72 nM).<sup>4</sup> In particular,  $\text{Pb}^{2+}$  as a nonbiodegradable element in essence with a longer biological half-life, tends to bioaccumulate in the human body. It produces irreversible damages to immune and nerve systems, especially for children with more susceptible exposure and greater harm.<sup>1,5,6</sup> Therefore, it poses far-reaching adverse impacts on public health even at ultratrace-level exposure.<sup>7,8</sup> Lead contamination in the environment such as soil and water can easily transfer to food including livestock and poultry meat, eggs, and milk, leading to an abundant resource of leadpolluted food.<sup>9</sup> In consideration of the widespreading and high toxicity of  $\text{Pb}^{2+}$ , it is necessary to develop sensitive methods for quantitatively detecting  $\text{Pb}^{2+}$  to ensure food and environmental safety. The conventional  $\text{Pb}^{2+}$ -analytical techniques included inductively coupled plasma (ICP),<sup>10</sup> atomic absorption/ fluorescence spectroscopy,<sup>11,12</sup> and reversed-phase high-performance liquid chromatography (RP-HPLC).<sup>13</sup> These techniques confer a precise detection of  $\text{Pb}^{2+}$  while requiring sophisticated, high-cost equipment, and well-trained operators, which hamper their further development of on-site detection tools used in resource-constrained regions. A clustered regularly interspaced short palindromic repeat (CRISPR)-associated (CRISPR/Cas) system has been proven powerful in developing assays for nucleic acid biomarkers. The RNA-guided recognition enables the CRISPR tools to be highly specific, and the multiple turnover of collateral cleavage provides signal amplification that contributes to sensitivity improvement.<sup>14–17</sup> CRISPR-based nucleic acid detection has been widely applied in monitoring environmental and food safety, mainly targeting

pathogens<sup>18</sup> and genetically modified organisms.<sup>19</sup> To enhance the sensitivity, the CRISPR technologies are generally combined with isothermal amplification strategies, such as recombinase polymerase amplification<sup>18</sup> and loop-mediated isothermal amplification.<sup>20</sup> Using CRISPR tools to detect non-nucleic acid biomarkers, however, requires compatible biorecognition and signal transduction elements. DNAzyme has been reported to be highly specific for metal ion recognition. Particularly, we found that the 5'-part of the cleaved substrate by DNAzyme-catalyzing bears a 2'3'-cyclic phosphate at the 3'-terminus,<sup>21</sup> which can act as the activator for RNase activity of Csm6, a much simpler multisubunit single effector from type III-A CRISPR/Cas systems than Cas12 and Cas13.<sup>22-24</sup> The Cas13a tandem Csm6 assay is the only application of Csm6 so far;<sup>22,25</sup> therefore, the discovery of DNAzymes capable of cascading Csm6 substantially broadens the Csm6 toolbox. In recent years, assays based on CRISPR/Cas12a and DNAzyme have been used for amplified detection of metal ions, but the indispensable separation step made them incapable of a one tube homogeneous reaction, and the design of guide RNAs and DNAzyme probes could be complex and needs careful optimization.<sup>26-28</sup> Based on the discovery of the alternative activation strategy of Csm6, we used GR-5 DNAzyme to serve as the biorecognition for Pb<sup>2+</sup> and coupled Csm6 to further amplify the recognition event. The Csm6-DNAzyme tandem assay (termed cDNAzyme) allowed a separation-free, sensitive detection of lead contamination and the elimination of extra elaborate design of nucleic acid structures. Compared to the original GR-5 DNAzyme, the Csm6-DNAzyme tandem improved the sensitivity for detecting Pb<sup>2+</sup> by 6.1 times. In addition, we tested two representative types of Csm6 nucleases in the tandem reaction. Finally, we applied the cDNAzyme assay to estimate the lead bioaccumulation in mice. The proposed cDNAzyme assay could serve as a platform for monitoring lead pollution.

## Experimental Section.

**Materials and Reagents.** All the oligonucleotides (Table S1, in the Supporting Information) were synthesized by Sangon Biotech. (Shanghai, China). Oligonucleotides with modifications were purified by HPLC, while others only require PAGE purification. HEPES (pH 7.5),  $\text{MgCl}_2$ , KCl,  $\text{MnCl}_2$ ,  $\text{NiCl}_2$ ,  $\text{Cd}(\text{NO}_3)_2$ ,  $\text{Al}(\text{NO}_3)_3$ ,  $\text{CuSO}_4$ ,  $\text{CoCl}_2$ ,  $\text{ZnCl}_2$ ,  $\text{FeCl}_3$ , and  $\text{Pb}(\text{CH}_3\text{COO})_2$  were bought from Sigma-Aldrich (Beijing, China). Arsenic and mercury standard solution was obtained from National Center of Analysis and Testing for Nonferrous Metals and Electronic Materials (NCATN, China).  $\text{HNO}_3$  and  $\text{HClO}_4$  were purchased from equipment division. BALB/c mice were obtained from Dossy Experimental Animals Co., Ltd. (Chengdu, China). T4 polynucleotide kinase (T4 PNK, 10 U/ $\mu\text{L}$ ) was purchased from Thermo Fisher Scientific (Waltham, USA). Fresh eggs were purchased from a local supermarket, and tap water was collected from the laboratory.

**Protein Expression and Purification.** First, plasmids containing DNA sequences encoding for *Thermus thermophilus* Csm6 (TtCsm6) and *Enterococcus italicus* (EiCsm6) were constructed and sequenced by Sangon Biotech (Shanghai, China), their sequences are listed in Table S2 (in the Supporting Information), and their plasmid vectors are shown in Figures S1 and S2 (in the Supporting Information). Next, the plasmids corresponding to TtCsm6 and EiCsm6 were transformed into *Escherichia coli* (BL21 Rosetta2 (DE3)), followed by growing in LB medium supplemented with chloramphenicol and kanamycin at an appropriate concentration. Then, protein expression was triggered by the addition of 0.2 mM IPTG (isopropyl- $\beta$ -D-thiogalactopyranoside), and the reaction was incubated at 18 °C for 16 h. Cells that have expressed proteins were harvested and resuspended in a lysis buffer containing 20 mM Tris-HCl pH 8.0, 300 mM KCl, and 10% glycerol. Following the filtration of cleared lysate on a 5 mL Ni-NTA cartridge (GE Healthcare), the column was washed with 10 column volumes of lysis buffer, and then the bound proteins were

eluted with five column volumes of lysis buffers. Dialysis of eluted proteins was executed overnight using storage buffer containing 20 mM HEPES (pH 7.5), 300 mM KCl, 5 mM MgCl<sub>2</sub>, and 10% glycerol in the presence of tobacco etch virus protease. Flow-through fractions were obtained via passing the dialyzed proteins through a 5 mL NiNTA cartridge, followed by concentration and further purification by size-exclusion chromatography using an S200 (16/600) column (GE Healthcare) in storage buffer. Finally, concentration of purified proteins was performed on 30,000 molecular weight cut-off centrifugal filters (Merck Millipore) and reached 5–75 mg/mL, and purified proteins were analyzed by SDS-PAGE using 12.5% polyacrylamide and Coomassie blue staining (Figure S3, in the Supporting Information), subsequently flash-frozen in liquid nitrogen and stored in a –80 °C refrigerator.

**Two-Step cDNAzyme Assay for Pb<sup>2+</sup> Detection.** First, the DNAzyme cutting reaction was performed in a 36 µL volume containing 1× buffer (20 mM HEPES, pH 7.5, 50 mM KCl, 5 mM MgCl<sub>2</sub>), 400 nM substrate strand (**Sub**), 400 nM DNAzyme strand (**Dz**), and Pb<sup>2+</sup> solution with various concentrations at 25 °C for 1 h. Subsequently, the cutting fragments can serve as the activators for Csm6 endoribonuclease; 4 µL of reporting mixture containing 100 nM Csm6 and 400 nM C5 reporter was added into the above reaction solution followed by incubation at 37 °C for 30 min. The fluorescence signal was finally recorded on a microplate reader Synergy H1 (BioTek, USA), with the excitation wavelength of 480 nm and emission ranging from 510 to 600 nm.

**One-Step cDNAzyme Assay for Pb<sup>2+</sup> Detection.** The reaction was performed in a 40 µL volume containing 1× buffer (20 mM HEPES, pH 7.5, 50 mM KCl, 5 mM MgCl<sub>2</sub>), 400 nM Sub, 400 nM Dz, 100 nM Csm6, 400 nM C5 reporter and Pb<sup>2+</sup> solution with various concentrations at 25 °C for 2 h, followed with fluorescence measurement.

**Lead Bioaccumulation in Mice.** All experimental animals (10 mice) were group-housed in a barrier facility and divided into two groups (gavage with  $\text{Pb}^{2+}$  and sterile PBS). Healthy mice (BALB/c, 6–8 weeks old) without pathogenic infection were first applied to adaptive feeding for 3 days; subsequently, oral gavage with bacteria-free  $\text{Pb}^{2+}$  solution (1000 mg/kg) or sterile PBS was performed thrice for 3 days. After euthanasia of the infection mice, kidney, liver, colon, and feces were harvested and weighed and then digested for later analysis.

**Sample Pretreatment.**  $\text{Pb}^{2+}$ -contaminated tap water, fresh eggs and groups of mice were first digested before detection using the cDNAzyme assay. Taking 0.1–0.5 g samples with different amounts of  $\text{Pb}^{2+}$  were added in an acid solution containing 10 mL of concentrated  $\text{HNO}_3$  and 5 mL of  $\text{HClO}_4$ , the incubation procedure was set to 180 °C, 40 min; 200 °C, 4 h; and 220 °C, 1 h, and the reaction was performed in a fume hood. Digested solutions were dissolved in an 8 mL volume of ultrapure water and adjusted to pH 7 using 1 M NaOH and 0.1 M HCl and finally making a constant volume of 13 mL, which can be used for later analysis.

## Results and Discussion

**Working Principle.** The cDNAzyme assay proceeds in two sequential reactions: DNAzyme cutting for  $\text{Pb}^{2+}$  recognition and CRISPR reporting for signal amplification (Figure 1). The DNAzyme composes of two strands: a substrate strand (**Sub**) modified with four riboadenosines at the 5'-terminus and a DNAzyme strand (**Dz**) free of any modification. DNAzyme cutting allows for synchronously implementing the recognition of  $\text{Pb}^{2+}$  and the following catalytic cleavage of **Sub**. The DNAzyme-catalyzing cleavage can produce a 5'-fragment terminated with 2',3'-cyclic phosphate,<sup>29</sup>  $\text{A4} > \text{p}$ , which can serve as the activator for Csm6 to initiate the subsequent CRISPR reporting.<sup>24</sup> The activated Csm6 presents a high endoribonuclease activity for indiscriminately cleaving collateral ssRNA reporters. In particular, it is reported that blocking activator degradation



could maintain the activation of Csm6 in a high level. A single 2'-fluoro (2'-F) modification at the second riboadenosine (rA2 nucleotide) of A4 > p showed the best blocking effect compared to other previously reported modifications.<sup>22</sup> Therefore, we modified a 2'-F at the rA2 nucleotide of the **Sub**. In addition, cytidine-homopolymer is one of the preferred substrates for the collateral cleavage of activated Csm6. We synthesized a poly C sequence modified with a fluorophore and quencher as the reporter of Csm6 (C5reporter).<sup>25</sup> Based on the principle, Pb<sup>2+</sup> can be recognized by the DNAzyme, followed by amplification using the Csm6- DNAzyme tandem, resulting in a sensitive assay for detecting Pb<sup>2+</sup>. The catalyzing cleavage of the **Sub** by **Dz** used in the cDNAzyme assay was tested using electrophoresis. Also, the original GR-5 DNAzyme was also tested as a comparison. Both DNAzymes could efficiently cleave the substrates (Figure 2A). The band (lane 2 or 7) loading with Sub-Dz duplex lagged behind compared to that with only Dz or Dz-O (Dz for original GR-5 DNAzyme) (lane 3 or 6) and Sub or Sub-O (Sub for original GR-5 DNAzyme) (lane 4 or 5), suggesting the hybridization between **Sub** and **Dz**. A further addition of Pb<sup>2+</sup> makes the band move forward (lane 1 or 8), indicating the cutting of **Sub** induced by Pb<sup>2+</sup>-activated Dz. The cleavage triggered dissociated **Sub** fragment (A4 > p) is too short relative to the **Sub-Dz** duplex, thus only resulting in a faint forward movement of the band in lane 1. Fluorescence analysis was performed to investigate the activation of Csm6 (Figure 2B). In the absence of Pb<sup>2+</sup>, negligible increases in fluorescence occurred when adding Csm6, **Sub**, and **Dz** compared with the blank fluorescence of the C5 reporter alone (Figure 2B, inset). Also, dramatic fluorescence enhancement (from 2456 to 65,750 at the maximum emission wavelength of 520 nm) was generated in the presence of Pb<sup>2+</sup>, suggesting the efficient Pb<sup>2+</sup>-specific cleavage. Given that blocking activator degradation could dramatically improve the collateral cleavage of Csm6,<sup>22</sup> we modified bases with 2'-F, 2'-H or 2'-O-methyl (2'- OMe) at different riboadenosines to investigate

the blocking effect (Figure 2C). The modification at the rA4 nucleotide was not considered due to its indispensability for DNAzyme cutting.<sup>30</sup> Inserting modification into rA2 and rA3 nucleotides could effectively block the degradation, and the 2'-F modification at rA2 showed the best blocking effect compared to others (Figure 2D). Also, this result was consistent with the previous report.<sup>22</sup> In addition, we found that the 2'-F-modified A4 activator terminated with hydroxyl (using T4 PNK to remove the 2',3'-cyclic phosphate) yielded a dramatic reduction of capacity for activating Csm6 (Figure 2E). Furthermore, we investigated the response of the cDNAzyme assay toward  $Pb^{2+}$  using two types of Csm6 nucleases (Figure 2F). The use of TtCsm6 where  $Pb^{2+}$ -specific DNAzyme cleavage generated activators resulted in a 3.5 times higher signal-to-background ratio than that using EiCsm6. The longer oligoadenylate activator is more susceptible to nucleolytic degradation by Csm6.<sup>22</sup> Different from TtCsm6, EiCsm6 recruits A6 > p as the activating ligand. Optimization of the cDNAzyme Assay. The key mechanism of the cDNAzyme assay lies in the dual cleavage of DNAzyme cutting and CRISPR reporting, which both are highly affected by the hybridization of Sub-Dz. 31 Twelve Dzs with varying arm lengths were designed (Figure S4, in the Supporting Information). We found that shortening the 3'-arm length from 14 to 10 nucleotide (nt) and of 5'-arm from 13 to 10 nt would lead to the strongest fluorescence, while further shortening would result in weak formation of Sub-Dz duplex. This indicated that nonstable hybridization or excessive stable hybridization between Dz and Sub both can reduce the multiple-turnover of the cleavage reaction. We further investigated the impact of the concentration of the Sub bearing preactivator, concentration of Csm6, and the ratio between Sub and Dz on the cDNAzyme assay (Figures S5 and S6A, in the Supporting Information). The highest output signal occurred at the Sub concentration of 400 nM, Csm6 concentration of 100 nM, and the ratio of Sub to Dz of 1:1 while retaining a low level of background. Temperature and pH can affect the stability of proteases

and their preference for attack sites on nucleic acid.<sup>32</sup> The investigation of reaction pH, temperature, and time showed that the highest signal to background ratio was achieved when using pH 7.5, performing DNAzyme cutting at 25 °C for 60 min and CRISPR reporting at 37 °C for 30 min (Figures S6B, S7, and S8, in the Supporting Information). Detection Performance of the cDNAzyme Assay. Under the optimal assaying conditions, a series of amount of standard Pb<sup>2+</sup> solution was used to test the detection performance of the two-step and one-step cDNAzyme assays, and the original GR-5 DNAzyme was performed as a comparison (Figure 3). The fluorescence of the three assays grew gradually along with the increase in the amount of Pb<sup>2+</sup> (0–200 nM) (Figure 3A–C). A linear regression equation for the two-step cDNAzyme assay could be obtained when target Pb<sup>2+</sup> fell in the concentration ranging from 0.1 to 100 nM and calculated as  $y = 554.55x + 3090.30$  ( $R^2 = 0.9972$ ), where y, x, and R represent the fluorescence response, Pb<sup>2+</sup> amounts, and correlation coefficient, respectively. Benefitting from the signal amplification, the cDNAzyme assay confers a high sensitivity with a limit of detection (LOD) of 70 pM (Figure 3D), allowing to meet the requirement for the maximum Pb<sup>2+</sup>-contamination level in drinking water (72 nM) defined by the USA EPA.<sup>33</sup> We defined LOD as the Pb<sup>2+</sup> concentration corresponding to the fluorescence output of the lowest limit of the linear ranges with the addition of 3-fold standard deviation. The dual cleavage conferred a high sensitivity of the cDNAzyme assay (Table S4, in the Supporting Information). In contrast, the original GR-5 DNAzyme exhibited a much narrower linear range, 0.5–25 nM, and a ~6.1 times higher LOD (430 pM) than the cDNAzyme assay (Figure 3E). The direct oligoadenylate-triggered activation of Csm6 could potentially eliminate the separation step and enable a one-tube homogeneous reaction. Therefore, we further explored the quantification performance of mix-and-read detection of the Csm6-DNAzyme tandem assay. The cDNAzyme assay allowed one-step detection at room temperature

(25 °C) (Figure 3F). Under the optimal conditions (Figures S4–S9, in the Supporting Information), the mix-and-read assay yielded an LOD of 4.951 nM, which meets the requirement for the maximum Pb<sup>2+</sup>-contamination level in drinking water (72 nM) suggested by the USA EPA. The trade-off in sensitivity of the one-step cDNAzyme assay compared to the two-step one may be due to the weaker turnover cleavage activity of Csm6 at 25 °C than that at 37 °C. We further investigated the specificity of the cDNAzyme assay for detecting Pb<sup>2+</sup>. Ten other metal ions containing Mn<sup>2+</sup>, Ni<sup>2+</sup>, Cd<sup>2+</sup>, Al<sup>3+</sup>, Cu<sup>2+</sup>, Co<sup>2+</sup>, Zn<sup>2+</sup>, Hg<sup>2+</sup>, Fe<sup>3+</sup>, and As<sup>3+</sup> were selected and tested at three gradient concentrations (10, 100, and 1000 nM). No metal ions led to a non-negligible fluorescence change compared with blank control except Pb<sup>2+</sup> (Figure 4), indicating the capability of the cDNAzyme assay to discriminate Pb<sup>2+</sup> in interference surroundings. The specific discriminability for Pb<sup>2+</sup> was mainly derived from the GR-5 DNAzyme.<sup>30</sup> T-Hg<sup>2+</sup>-T complex hindered the binding of the ployT arm of Dz with Sub, <sup>34</sup> further reducing the fluorescence responses induced by Hg<sup>2+</sup> compared to other interference metal ions.

**Monitoring Lead Pollution in Water and Food Samples.** Heavy metals have polluted approximately 40% of water resources of the planet.<sup>35</sup> Therefore, we investigated the performance of the proposed cDNAzyme assay for determining lead contamination in water. We employed the cDNAzyme assay to analyze the water spiked with various Pb<sup>2+</sup> concentrations (10, 30, and 50 nM). The obtained recovery of Pb<sup>2+</sup> determination in water fell in the value ranging from 90.29 to 112.17%, and the relative standards (RSD) remained within 3.14% (Table S3, in the Supporting Information). In addition, the metal accumulation in soil and water can further transfer into the bodies of poultry grown in the environment. The test results of lead contamination in fresh egg, a common poultry product, showed recoveries ranging from 90.09 to 105.32% with RSDs of 1.51–3.12% (Table S3, in the Supporting Information). These results demonstrated that the

potential application of the cDNAzyme assay for determining lead contamination in food and the environment.

**Estimating the Lead Bioaccumulation in Mice.** Practically, the cDNAzyme assay was further challenged to serve as a tool for estimating the lead bioaccumulation in mice.  $\text{Pb}^{2+}$  is a toxic metal contaminant that can enter and ultimately accumulate into the body, causing adverse health damages even at low exposure levels. We here selected mice with acute lead exposure as the model. Adult mice were first treated with adaptive feeding for 2 days and were then acutely and orally exposed to  $\text{Pb}^{2+}$  at a concentration of 1000 mg/kg for 3 days, followed by dissection to harvest groups of kidney, liver, colon, and feces and later performing digestion (Figure 5A). Intestine, kidney and liver are the main organs closely related to lead excretion.<sup>36</sup> We parallelly employed the cDNAzyme assay and ICP testing to estimate the  $\text{Pb}^{2+}$  bioaccumulation in mice. Figure 5B,C illustrates that acute lead exposure leads to the accumulation of  $\text{Pb}^{2+}$  in tissues in all groups. Accumulation levels of in vivo tissues are in the order of colon (138.5  $\mu\text{g/g}$  wet tissue,  $n = 5$ ) > kidney (128.1  $\mu\text{g/g}$  wet tissue,  $n = 5$ ) > liver (21.2  $\mu\text{g/g}$  wet tissue,  $n = 5$ ) and are significantly lower than that in fecal excretion (25639.0  $\mu\text{g/g}$  wet feces,  $n = 5$ ). The results of our cDNAzyme measurements of distribution of lead ions in mouse organs are in good accordance with a previous report,<sup>37</sup> and the trend is similar to the lead bioaccumulation in rats.<sup>38</sup> We found that most of the  $\text{Pb}^{2+}$  was excreted. However, there are higher accumulation levels in the colon and kidney than in the liver. It may be because lead excretion in urine and feces, which are the main pathways, requires passage through the kidney and intestine. Additionally, we have fitted the relationship between the  $\text{Pb}^{2+}$  content calculated using the cDNAzyme assay and that using ICP testing, and a linear regression line ( $y = 0.8702$ ,  $R^2 = 0.90183$ ) was obtained, demonstrating the consistency of the two methods (Figure 5D).

## Conclusions

In summary, we reported a cascade assay via using DNzyme cutting in tandem with CRISPR reporting, enabling one-pot and sensitive detection of lead pollution. The coupling with Csm6 with DNzyme eliminates the complex design and optimization of guide RNAs. The signal amplification derived from CRISPR reporting conferred ~6.1 times higher sensitivity than the original GR-5 DNzyme assay. In particular, the cDNzyme assay allowed for one-step, mix-and-read detection at room temperature. The tandem assay enabled a high specificity for detecting Pb<sup>2+</sup> in the presence of other interfering ions including Mn<sup>2+</sup>, Ni<sup>2+</sup>, Cd<sup>2+</sup>, Al<sup>3+</sup>, Cu<sup>2+</sup>, Co<sup>2+</sup>, Zn<sup>2+</sup>, Hg<sup>2+</sup>, Fe<sup>3+</sup>, and As<sup>3+</sup> and allowed to precisely detect lead pollution in water and food samples. In addition, the assay allowed for the estimation of lead accumulation in mice and revealed that the colon and kidney were more susceptible to lead accumulation than the liver. These results indicated that the cDNzyme assay would be used in monitoring lead pollution-associated environmental and biosafety issues.

## Acknowledgements

This work was financially supported by National Natural Science Foundation of China (no. 22074100), the Young Elite Scientist Sponsorship Program by CAST (no.YESS20200036), the Green Manufacturing Project of Ministry of Industry and Information Technology of China, and the Researchers Supporting Project (no. RSP-2021/138), King Saud University, Riyadh, Saudi Arabia. We thank Dr. Xi Wu from Analytical & Testing Center, Sichuan University for the measurement of lead in tissue samples using inductively coupled plasma.

## References

- (1) Zapata, F.; Caballero, A.; Espinosa, A.; Tárraga, A.; Molina, P. *Org. Lett.* **2008**, 10, 41–44.
- (2) Zhang, X.; Huang, X.; Xu, Y.; Wang, X.; Guo, Z.; Huang, X.; Li, Z.; Shi, J.; Zou, X. *Biosens. Bioelectron.* **2020**, 168, No. 112544.
- (3) Huang, Y.; Keller, A. A. *Water Res.* **2015**, 80, 159–168.
- (4) Guo, Y.; Li, J.; Zhang, X.; Tang, Y. *Analyst* **2015**, 140, 4642–4647.
- (5) Wu, Y.; Shi, Y.; Deng, S.; Wu, C.; Deng, R.; He, G.; Zhou, M.; Zhong, K.; Gao, H. *Food Chem.* **2021**, 343, No. 128425.
- (6) Xu, J.; Liu, M.; Zhao, W.; Wang, S.; Gui, M.; Li, H.; Yu, R. *J. Hazard. Mater.* **2022**, 429, No. 128347.
- (7) Wang, F.; Zhang, Y.; Lu, M.; Du, Y.; Chen, M.; Meng, S.; Ji, W.; Sun, C.; Peng, W. *Sens. Actuators, B* **2021**, 337, No. 129816.
- (8) Han, S.; Zhou, X.; Tang, Y.; He, M.; Zhang, X.; Shi, H.; Xiang, Y. *Biosens. Bioelectron.* **2016**, 80, 265–272.
- (9) Uchimiya, M.; Bannon, D.; Nakanishi, H.; McBride, M. B.; Williams, M. A.; Yoshihara, T. *J. Agric. Food Chem.* **2020**, 68, 12856–12869.
- (10) Lin, C.-H.; Chen, Y.; Su, Y.-A.; Luo, Y.-T.; Shih, T.-T.; Sun, Y.-C. *Anal. Chem.* **2017**, 89, 5891–5899.
- (11) Endah, N.; Surantaatmadja, S. I. *J. Phys.: Conf. Ser.* **2019**, 1179, No. 012178.

- (12) Malik, L. A.; Bashir, A.; Qureashi, A.; Pandith, A. H. *Environ. Chem. Lett.* **2019**, 17, 1495–1521.
- (13) Yang, G.; Zhang, C.; Hu, Q.; Yin, J. *J. Chromatogr. Sci.* **2003**, 41, 195–199.
- (14) Wu, L.; Zhou, T.; Huang, R. *Sens. Actuators, B* **2022**, 357, No. 131411.
- (15) Ke, Y.; Ghalandari, B.; Huang, S.; Li, S.; Huang, C.; Zhi, X.; Cui, D.; Ding, X. *Chem. Sci.* **2022**, 13, 2050–2061.
- (16) Xue, T.; Lu, Y.; Yang, H.; Hu, X.; Zhang, K.; Ren, Y.; Wu, C.; Xia, X.; Deng, R.; Wang, Y. *J. Agric. Food Chem.* **2022**, 70, 1670–1678.
- (17) Yang, H.; Chen, J.; Yang, S.; Zhang, T.; Xia, X.; Zhang, K.; Deng, S.; He, G.; Gao, H.; He, Q.; Deng, R. *Anal. Chem.* **2021**, 93, 12602–12608.
- (18) Jiao, J.; Yang, M.; Zhang, T.; Zhang, Y.; Yang, M.; Li, M.; Liu, C.; Song, S.; Bai, T.; Song, C.; Wang, M.; Pang, H.; Feng, J.; Zheng, X. *J. Hazard. Mater.* **2022**, 426, No. 128038.
- (19) Zhu, X.; Yang, H.; Wang, M.; Wu, M.; Khan, M. R.; Luo, A.; Deng, S.; Busquets, R.; He, G.; Deng, R. *ACS Synth. Biol.* **2022**, 11, 317–324.
- (20) Broughton, J. P.; Deng, X.; Yu, G.; Fasching, C. L.; Servellita, V.; Singh, J.; Miao, X.; Streithorst, J. A.; Granados, A.; Sotomayor Gonzalez, A.; Zorn, K.; Gopez, A.; Hsu, E.; Gu, W.; Miller, S.; Pan, C.-Y.; Guevara, H.; Wadford, D. A.; Chen, J. S.; Chiu, C. Y. *Nat. Biotechnol.* **2020**, 38, 870–874.
- (21) Micura, R.; Höbartner, C. *Chem. Soc. Rev.* **2020**, 49, 7331–7353.
- (22) Liu, T. Y.; Knott, G. J.; Smock, D. C. J.; Desmarais, J. J.; Son, S.; Bhuiya, A.; Jakhanwal, S.; Prywes, N.; Agrawal, S.; Díaz De León Derby, M.; Switz, N. A.; Armstrong, M.; Harris, A.



R.; Charles, E. J.; Thornton, B. W.; Fozouni, P.; Shu, J.; Stephens, S. I.; Kumar, G. R.; Zhao, C.; et al. *Nat. Chem. Biol.* **2021**, 17, 982–988.

(23) Niewoehner, O.; Garcia-Doval, C.; Rostøl, J. T.; Berk, C.; Schwede, F.; Bigler, L.; Hall, J.; Marraffini, L. A.; Jinek, M. *Nature* **2017**, 548, 543–548.

(24) Jia, N.; Jones, R.; Yang, G.; Ouerfelli, O.; Patel, D. J. *Mol. Cell* 2019, 75, 944–956.e6.

(25) Gootenberg Jonathan, S.; Abudayyeh Omar, O.; Kellner Max, J.; Joung, J.; Collins James, J.; Zhang, F. *Science* **2018**, 360, 439–444.

(26) Li, J.; Yang, S.; Zuo, C.; Dai, L.; Guo, Y.; Xie, G. *ACS Sens.* **2020**, 5, 970–977.

(27) Xiong, Y.; Zhang, J.; Yang, Z.; Mou, Q.; Ma, Y.; Xiong, Y.; Lu, Y. *J. Am. Chem. Soc.* **2020**, 142, 207–213.

(28) Li, Y.-Y.; Li, H.-D.; Fang, W.-K.; Liu, D.; Liu, M.-H.; Zheng, M.-Q.; Zhang, L.-L.; Yu, H.; Tang, H.-W. *ACS Sens.* **2022**, 7, 1572–1580.

(29) McConnell, E. M.; Cozma, I.; Mou, Q.; Brennan, J. D.; Lu, Y.; Li, Y. *Chem. Soc. Rev.* **2021**, 50, 8954–8994.

(30) Lan, T.; Furuya, K.; Lu, Y. *Chem. Commun.* **2010**, 46, 3896–3898.

(31) Yang, Y.; Yang, H.; Wan, Y.; Zhou, W.; Deng, S.; He, Y.; He, G.; Xie, X.; Deng, R. *J. Hazard. Mater.* **2021**, 413, No. 125383.

(32) Kamman, J. F.; Tatini, S. R. *J. Food Sci.* **1977**, 42, 421–424.

(33) Ren, W.; Zhang, Y.; Fan, Y. Z.; Dong, J. X.; Li, N. B.; Luo, H. Q. *J. Hazard. Mater.* **2017**, 336, 195–201.

- (34) Wang, S.; Lin, B.; Chen, L.; Li, N.; Xu, J.; Wang, J.; Yang, Y.; Qi, Y.; She, Y.; Shen, X.; Xiao, X. *Anal. Chem.* **2018**, 90, 11764–11769.
- (35) Zhou, Q.; Yang, N.; Li, Y.; Ren, B.; Ding, X.; Bian, H.; Yao, X. *Glob. Ecol. Conserv.* **2020**, 22, No. e00925.
- (36) Goyer, R. A.; Mahaffey, K. R. *Environ. Health Perspect.* **1972**, 2, 73–80.
- (37) Yu, Y.; Yu, L.; Zhou, X.; Qiao, N.; Qu, D.; Tian, F.; Zhao, J.; Zhang, H.; Zhai, Q.; Chen, W. J. *Trace Elem. Med. Biol.* **2020**, 62, No. 126624.
- (38) Sadykov, R.; Digel, I.; Artmann, A.; Uuml, L. T.; Porst, D.; Linder, P.; Kayser, P.; Artmann, G.; Savitskaya, I.; Zhubanova, A. *J. Occup. Health* **2009**, 51, 64–73

## Graphical abstract

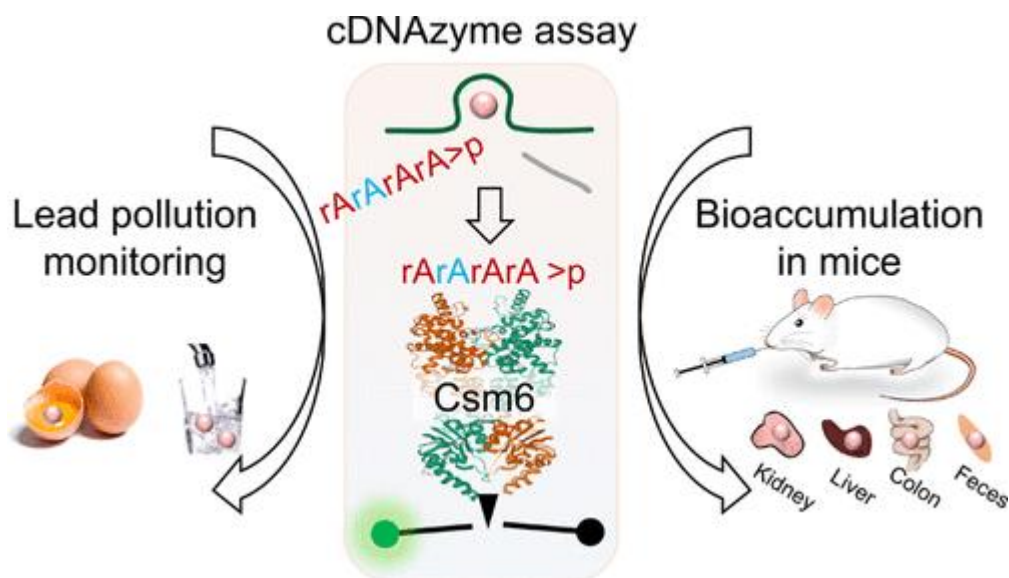


Figure 1. Working principle of the cDNAzyme assay for  $Pb^{2+}$  detection and its application for the investigation of bioaccumulation in mice.

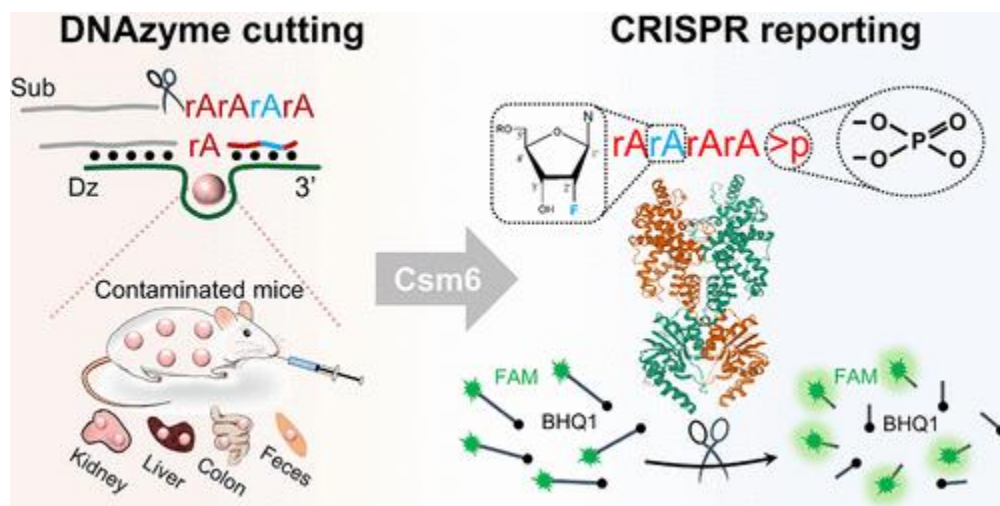


Figure 2. Investigation of the working principle of the cDNAzyme assay for  $\text{Pb}^{2+}$  detection. (A) Electrophoresis analysis of the cDNAzyme assay and original GR-5 DNAzyme response to  $\text{Pb}^{2+}$ . (B) Fluorescence response of the cDNAzyme assay toward  $\text{Pb}^{2+}$ . (C) Design of chemical modifications at different riboadenosines of **Sub**. (D) Fluorescence response corresponding to the different chemical modifications at **Sub**. (E) Fluorescence response of the cDNAzyme assay using different activators, including A4 > p, A4 > p, and A4-OH both with a 2'-F modification at the rA2 nucleotide. The A4-OH was obtained by dephosphorylation of A4 > p using T4 PNK. (F) Fluorescence response of the cDNAzyme assay toward  $\text{Pb}^{2+}$  using TtCsm6 and EiCsm6 nucleases. The blue marked letter represents the ribonucleotide with 2'-F modification. The excitation wavelength was 480 nm with an emission of 510–600 nm. The concentrations of  $\text{Pb}^{2+}$ , **Sub** or **Sub-O**, **Dz** or **Dz-O**, TtCsm6 or EiCsm6, and C5 reporter were 150, 400, 400, 100, and 400 nM, respectively.

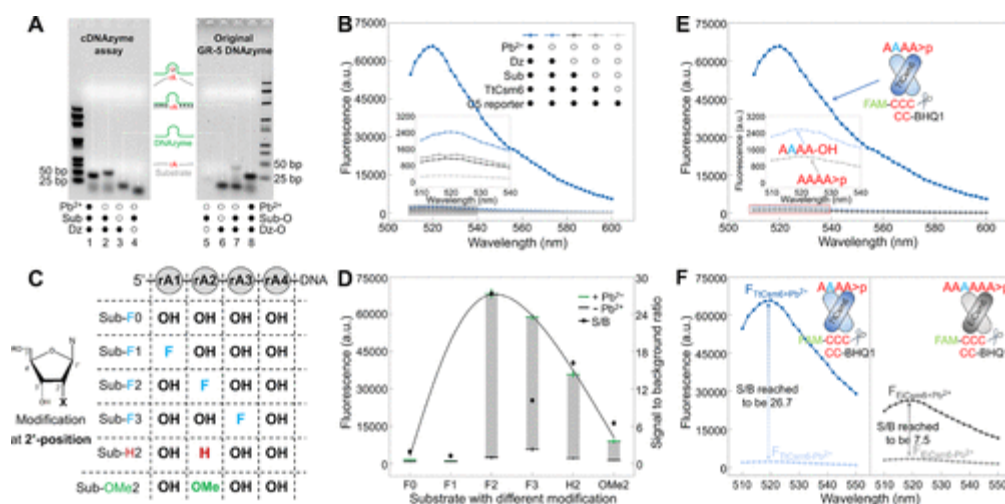


Figure 3. Investigation of the quantification performance for  $\text{Pb}^{2+}$  detection. Fluorescence spectra of the two-step cDNAzyme assay (A), the original GR-5 DNAzyme (B), and the one-step cDNAzyme assay (C) upon the addition of  $\text{Pb}^{2+}$  at various concentrations (0, 0.1, 0.5, 1, 5, 10, 25, 50, 100, 150, and 200 nM for (A and C); 0, 0.5, 1, 5, 10, 25, 50, 100, 150, and 200 nM for (B)). Calibration curve using the two-step cDNAzyme assay (D), the original GR-5 DNAzyme (E), and the one-step cDNAzyme assay (F) for determining the different concentrations of  $\text{Pb}^{2+}$ . Inset: linear relationship between the output fluorescence signal and  $\text{Pb}^{2+}$  concentration.

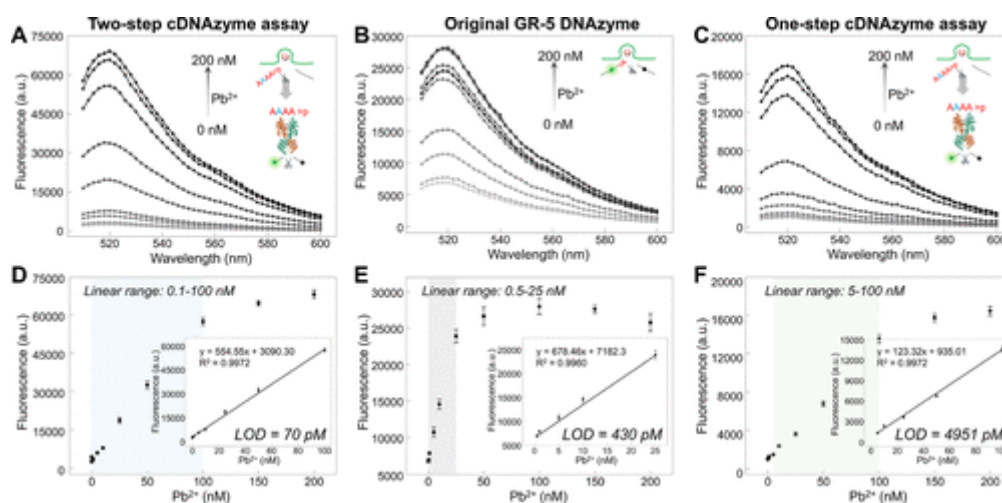


Figure 4. Specificity test of the cDNAzyme assay. The fluorescence response to the addition of  $\text{Pb}^{2+}$  and other metal ions. The gradient concentrations were set to 10, 100, and 1000 nM.

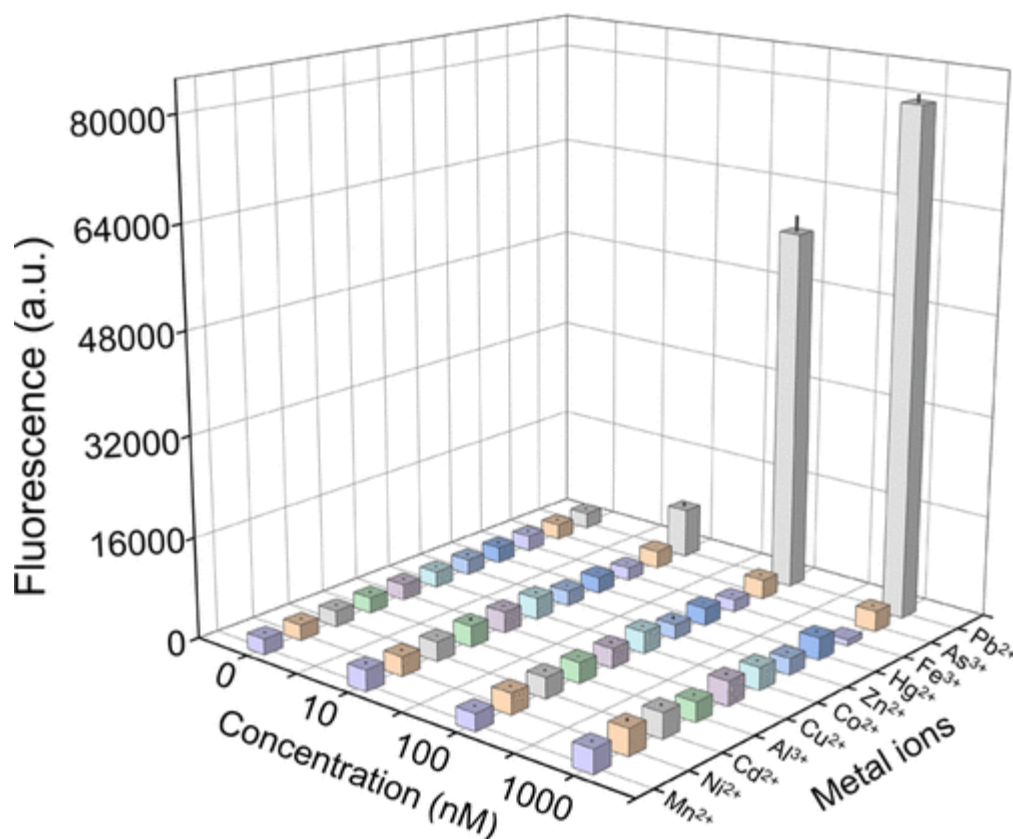
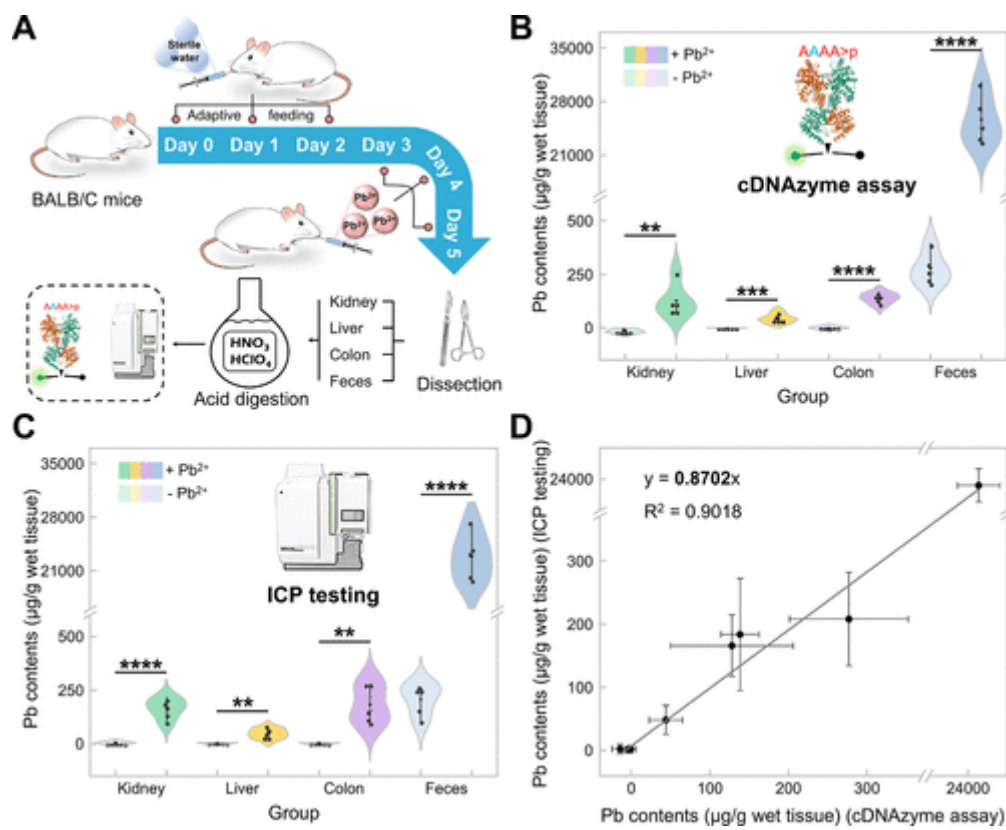


Figure 5. Estimating the bioaccumulation of  $\text{Pb}^{2+}$  in mice parallelly using the cDNAzyme assay and ICP testing. (A) Schematic illustrating the animal study protocol. Experimental mice were categorized into two groups: control (treated with sterile PBS) and bacteria-free  $\text{Pb}^{2+}$  solution (1000 mg/kg) ( $n = 5$  each group). (B) Analyzing  $\text{Pb}^{2+}$  content using the cDNAzyme assay in different infected groups of mice with different concentrations of  $\text{Pb}^{2+}$  (control, 1000 mg/kg;  $n = 5$ ). (C) Analyzing  $\text{Pb}^{2+}$  content using ICP testing in different infected groups of mice with different concentrations of  $\text{Pb}^{2+}$  (control, 1000 mg/kg;  $n = 5$ ). (D) Relationship of  $\text{Pb}^{2+}$  content calculated using ICP testing toward that using the cDNAzyme assay. All of the tests were performed as five replicates (two-tailed Student's  $t$  test; \*\*\*\* $P < 0.0001$ , \*\*\* $P < 0.001$ , \*\* $P < 0.01$ ,  $0.01 < *P < 0.05$ , ns,  $P > 0.05$ ).



## Supporting information

### **Csm6-DNAzyme tandem assay for one-pot and sensitive analysis of lead pollution and bioaccumulation in mice**

Hao Yang<sup>a</sup>, Feng Li<sup>b</sup>, Ting Xue<sup>a</sup>, Mohammad Rizwan Khan<sup>d</sup>, Xuhan Xia<sup>a</sup>, Rosa Busquets<sup>e</sup>, Hong Gao<sup>a,\*</sup>, Yi Dong<sup>a</sup>, Wenhui Zhou<sup>c</sup>, Ruijie Deng<sup>a,\*</sup>

<sup>a</sup> *College of Biomass Science and Engineering, Sichuan University, Chengdu 610065, China*

<sup>b</sup> *Key Laboratory of Green Chemistry & Technology of Ministry of Education, College of Chemistry, Analytical & Testing Center, Sichuan University, Chengdu, Sichuan 610065, China*

<sup>c</sup> *Xiangya School of Pharmaceutical Sciences, Central South University, Changsha, Hunan 410013, China*

<sup>d</sup> *Department of Chemistry, College of Science, King Saud University, Riyadh, 11451, Saudi Arabia*

<sup>e</sup> *School of Life Sciences, Pharmacy and Chemistry, Kingston University London, Penrhyn Road, KT1 2EE, Kingston Upon Thames, United Kingdom*

\*e-mail:

Hong Gao, gao523@hotmail.com

Ruijie Deng, [drj17@scu.edu.cn](mailto:drj17@scu.edu.cn)



## Table of content

<b>Table S1.</b> Oligonucleotide sequences.....	S3
<b>Table S2.</b> Sequences of plasmids containing DNA sequences encoding for <i>Thermus thermophilus</i> Csm6 (TtCsm6) and <i>Enterococcus italicus</i> (EiCsm6).....	S4
<b>Table S3.</b> Detection of Pb <sup>2+</sup> spiked in the fresh egg and tap water samples.....	S5
<b>Table S4.</b> Comparisons of detection performance of different fluorescent assays.....	S6
<b>Figure S1.</b> Plasmid vector for expression of TtCsm6.....	S7
<b>Figure S2.</b> Plasmid vector for expression of EiCsm6.....	S8
<b>Figure S3.</b> SDS-PAGE analysis of purified Csm6 proteins.....	S9
<b>Figure S4.</b> Optimization of the lengths of two arms of DNAzyme strand.....	S10
<b>Figure S5.</b> Optimization of the concentration of substrate and TtCsm6.....	S11
<b>Figure S6.</b> Optimization of the amount of DNAzyme strand and buffer pH.....	S12
<b>Figure S7.</b> Optimization of the reaction temperature and time of DNAzyme cutting.....	S13
<b>Figure S8.</b> Optimization of the reaction temperature and time of CRISPR reporting.....	S14
<b>Figure S9.</b> Optimization of the one-step cDNAzyme assay for Pb <sup>2+</sup> detection.....	S15

**Table S1.** Oligonucleotide sequences

Number	Oligonucleotide	Sequences ( 5' to 3' )
1	Sub (Sub-F2)	<b>rArArArA</b> GGAAGTGGTAACGTCAATTG
2	Sub-E	<b>rArArArArArA</b> GGAAGTGGTAACGTCAATTG
3	Sub-F0	<b>rArArArA</b> GGAAGTGGTAACGTCAATTG
4	Sub-F1	<b>rArArArA</b> GGAAGTGGTAACGTCAATTG
5	Sub-F3	<b>rArArArA</b> GGAAGTGGTAACGTCAATTG
6	Sub-H2	<b>rArArArA</b> GGAAGTGGTAACGTCAATTG
7	Sub-OMe2	<b>rArArArA</b> GGAAGTGGTAACGTCAATTG
8	Dz-C 9-4t	GTTACCACT GAAGTAGCGCCGCCG TTTT
9	Dz-C 9-6t	GTTACCACT GAAGTAGCGCCGCCG TTTTTT
10	Dz-C 9-8t	GTTACCACT GAAGTAGCGCCGCCG TTTTTTTT
11	Dz-C 9-10t	GTTACCACT GAAGTAGCGCCGCCG TTTTTTTTTT
12	Dz-C 9-12t	GTTACCACT GAAGTAGCGCCGCCG TTTTTTTTTTTT
13	Dz-C 9-14t	GTTACCACT GAAGTAGCGCCGCCG TTTTTTTTTTTTTT
14	Dz-C 8-10t	TTACCACT GAAGTAGCGCCGCCG TTTTTTTTTT
15	Dz-C 10-10t	CGTTACCACT GAAGTAGCGCCGCCG TTTTTTTTTT
16	Dz-C 11-10t	ACGTTACCACT GAAGTAGCGCCGCCG TTTTTTTTTT
17	Dz-C 12-10t	GACGTTACCACT GAAGTAGCGCCGCCG TTTTTTTTTT
18	Dz-C 13-10t	TGACGTTACCACT GAAGTAGCGCCGCCG TTTTTTTTTT
19	Sub-O	ACTCAC /i <b>BHQ1d</b> T/ AT <b>rA</b> GGAAG /i <b>6FAMd</b> T/ GATGGACGTG
20	Dz-O	GTCCATCACT GAAGTAGCGCCGCCG TATAG
21	C5 reporter	<b>6FAM-rCrCrCrCrC-BHQ1</b>

\* The bold, red-marked letters represent the ribonucleotide at this position, the blue marked letters represent the ribonucleotides with 2'-F modification, the deep red marked letters represent the ribonucleotides with 2'-H, the green marked letters represent the ribonucleotides with 2'-OMe, and all other sequences are deoxyribonucleotides.

**Table S2.** Sequences of plasmids containing DNA sequences encoding for *Thermus thermophilus* Csm6 (TtCsm6) and *Enterococcus italicus* (EiCsm6)

Proteins	Sequences
TtCsm6	atggaagatctggatgcactgtgggaacgttaccgtgaagcgggtcgtgcaggcggtaacccgcaggcgt gtatcaggaaatggttggccggcgctgctggcgctgtggcgtgaaaaaccgcgtgtttaccggtccgcag gccttcgtgtctctgttcacaccctgggtaccagcccgaagcgaccgcgtggccatcctgggcgcgggc gctgaacgtgtttacgtgctgcacccccggaatccgcgcgttccgtccgcgctgcccaggacaccggt aaagacctgtacccggtggaaatcggtaaatctgatgtggaagcgattatcggaagttaaactgtgctgg aaaaacacccggaagtccggtggcactggatctgaccagcgggactaaagctatgtccgtggcctggcg gcagccggctcttctccagcgttttatccgaaagttcgtgtttacgtggataacgaggactacgatccgga actgcgccgtccgcgtgctggtaccgaaaaactgcgcacctgccgaacccgcacgaagcgctggcgga gtagatgcgtgttcgaaaaagaactctatggcaaaggtaattcggccaggccgcagcgtactccgcggt atggttggccgcaccggttaaccaggcgtagcactgtatgcgctgctggcagaaatgtaccgtgcatggcgt gcactggactttggtgaagccctgaaagcggggccgtaaatctctggccagctgagccagaacgtgtggtg aaccacccgctgaacgcccgcgtgaagcgctggaagcgcaggttgcctgctggaagcggtagatcgtt cctgaaagcccgcgacttcgctctgaaagaagggtgtttacggcctggcgctacgctgctgcacctggcaca ggaagctaaagaagaagcggcggtgctggccgcactgtatgcataccgcgctctggaactgctgctgcagg aacgtctggcgctgctgggcccgtgctgtaagctccgggtctgagcccgaagaagccgaagccctgcgt aaagctctggcggaactgctgggcgtcctgccggaagaagtgcgcctgccggcgaaactgggtctgctgga cctgctggcattcctgcgctgaaaggcgacgaagctctgggcccgtgagcctggctgaactgcgcggtctt gcaggcgcgctgaaaggctgtaactccgcgctgctggtgcacggctttgacgtgccgagcccgaagcagt agaaggcatcgacgcctggcgagggcctgctgcaggacctggaagcgcgacccgcgtgggtccgct gtctccggaaccggtgccgctgggttctaa atgaaaatctgttcagcccgatcggtaacaccgatccgtggcgcaacgatcgtgacggcgcgatgctgca catcgtgcgtcactaccagccggaccgtgtgttctgttttaccgaaagcatctggcagggttaaccagcactt ctccggccagcaggcggttcgattgggttaaaattatccagagcatcaacgaaaactgccagatcgaaatcaa atgcgacaccatcgaaagtgaaaacgacttcgatgcgtacaaagacctgttccaccagtagctgggtgaaga aaaacgtaaaatacccgaaacgcggaatctttctgaacgtgacctccggtacccgcagatggaaaccaccc tgtcctggaatacgttacctacccggacaaaatgcgctgcatccagggtgagcaccgcgtgaaaacctcta acgcgaaaactaaatatgcgcaggcggttgccaggaagttgatctggaaatcgtaacgaagaagaatct cagcagccgagccgttgccataaaatcgcatcctgtcttccgtgaagctatcgtgcgtaaccagatcaaat ccctgctggataactacgattacgaagcgccctgcagctggttgcgagccagaaatccttccgtaacggca aagaaatccgtaaaaaactgaaagaactgatcgtatgatataaaatgcaccgcgtgttcagctacctgatca aacagtatccgcgcaacgaaaaactgcagaaagcgtgctgcacaccatcctgctggaaatgcgccacca gcgcggtgacatcgcggaaccctgatccgtgtgaaaagcatcgcggaatacatcgttgaacagtacatcc agaaaaactatccgtacctgatcatctacaaagaagataaaaccgtacttcaacgtgagctacagccaggaa ctgaccgaatcttacctggcgctgatggactctcgtacaaagaaaaccaaaaaagatgaccgttgatagc ctggaccgtattctgggttcccggttaccgtgacttctgcagctgctggaagcgagcaacgaaatgacca acgaaatgaacaaagttaacgaaatcaacaacctgcgtacaaagtgcgcacaacctggactccctgaa cctggatcgtgataaaaacggctgtaaaatcaccaacgcggttaccgcggttctaccatgctgctggcggtt tcccggaagtgcaggaaaacgatttccactacctgaaacagtttaaccagttatcaaagaactgctgtaa
EiCsm6	atgaaaatctgttcagcccgatcggtaacaccgatccgtggcgcaacgatcgtgacggcgcgatgctgca catcgtgcgtcactaccagccggaccgtgtgttctgttttaccgaaagcatctggcagggttaaccagcactt ctccggccagcaggcggttcgattgggttaaaattatccagagcatcaacgaaaactgccagatcgaaatcaa atgcgacaccatcgaaagtgaaaacgacttcgatgcgtacaaagacctgttccaccagtagctgggtgaaga aaaacgtaaaatacccgaaacgcggaatctttctgaacgtgacctccggtacccgcagatggaaaccaccc tgtcctggaatacgttacctacccggacaaaatgcgctgcatccagggtgagcaccgcgtgaaaacctcta acgcgaaaactaaatatgcgcaggcggttgccaggaagttgatctggaaatcgtaacgaagaagaatct cagcagccgagccgttgccataaaatcgcatcctgtcttccgtgaagctatcgtgcgtaaccagatcaaat ccctgctggataactacgattacgaagcgccctgcagctggttgcgagccagaaatccttccgtaacggca aagaaatccgtaaaaaactgaaagaactgatcgtatgatataaaatgcaccgcgtgttcagctacctgatca aacagtatccgcgcaacgaaaaactgcagaaagcgtgctgcacaccatcctgctggaaatgcgccacca gcgcggtgacatcgcggaaccctgatccgtgtgaaaagcatcgcggaatacatcgttgaacagtacatcc agaaaaactatccgtacctgatcatctacaaagaagataaaaccgtacttcaacgtgagctacagccaggaa ctgaccgaatcttacctggcgctgatggactctcgtacaaagaaaaccaaaaaagatgaccgttgatagc ctggaccgtattctgggttcccggttaccgtgacttctgcagctgctggaagcgagcaacgaaatgacca acgaaatgaacaaagttaacgaaatcaacaacctgcgtacaaagtgcgcacaacctggactccctgaa cctggatcgtgataaaaacggctgtaaaatcaccaacgcggttaccgcggttctaccatgctgctggcggtt tcccggaagtgcaggaaaacgatttccactacctgaaacagtttaaccagttatcaaagaactgctgtaa

**Table S3.** Detection of Pb<sup>2+</sup> spiked in the fresh egg and tap water samples

Samples	Added (nM)	Found (nM)	Recovery (%)	RSD (%) n=3
Fresh egg	10	9.01	90.09	3.12
	30	27.13	90.43	1.51
	50	52.66	105.32	1.71
Tap water	10	9.34	93.42	2.35
	30	27.09	90.29	2.71
	50	56.09	112.17	3.14

**Table S4.** Comparisons of detection performance of different fluorescent assays for Pb<sup>2+</sup> sensing

Strategy	Recognition	One-step	One-tube	Separation required	Elaborate probe design	Linear range	LOD	Application	Ref.
<b>Csm6-DNAzyme tandem assay</b>	<b>DNAzyme</b>	<b>Yes</b>	<b>Yes</b>	<b>No</b>	<b>No</b>	<b>0.1-100 nM</b>	<b>70 pM</b>	<b>Water, eggs and mice</b>	<b>This work</b>
Magnetic separation-based Cas12a-DNAzyme	DNAzyme	No	No	Yes	Yes	0.01-10 nM	53 pM	Water	<i>ACS Sens.</i> , 2020, 5, 970-977
Cas12a/Cas14a-DNAzyme	DNAzyme	No	No	Yes	Yes	0.24-48 nM	480 pM	Water	<i>Anal. Chim. Acta</i> , 2022, 1192, 339356
Cas12a-G-quadruplex assay	G-quadruplex	No	Yes	No	No	0.1 nM- 5 µM	2.6 nM	Tea Beverage and milk	<i>Food Chem.</i> , 2022, 378, 131802
Cell-free paper-based biosensor	Allosteric transcription factor	No	Yes	No	No	1-250 nM	0.1 nM	Water	<i>J. Hazard. Mater.</i> , 2022, 438, 129499
Tetrahedral DNA Nanostructure-based DNAzyme	DNAzyme	Yes	Yes	No	Yes	0-500 nM	0.9125 nM	Tobacco leaf extracts	<i>J. Clean. Prod.</i> , 2022, 362, 132544
Label-free sequential DNAzyme	DNAzyme	No	Yes	No	Yes	0.1-10	0.22	Water and eggs	<i>ACS Sens.</i> , 2018, 3, 2660-2666

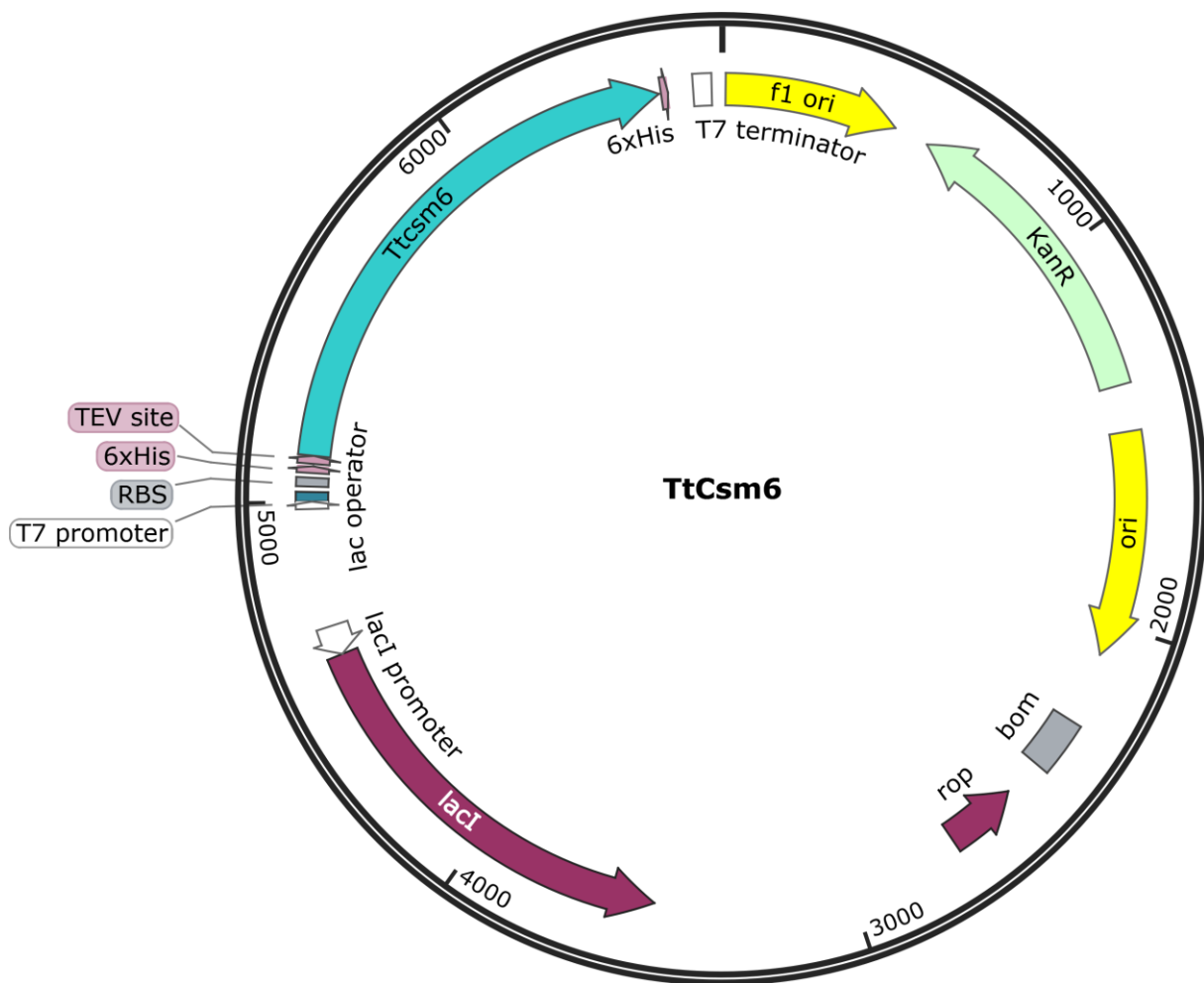


**Figure S1.** Plasmid vector for expression of TtCsm6.

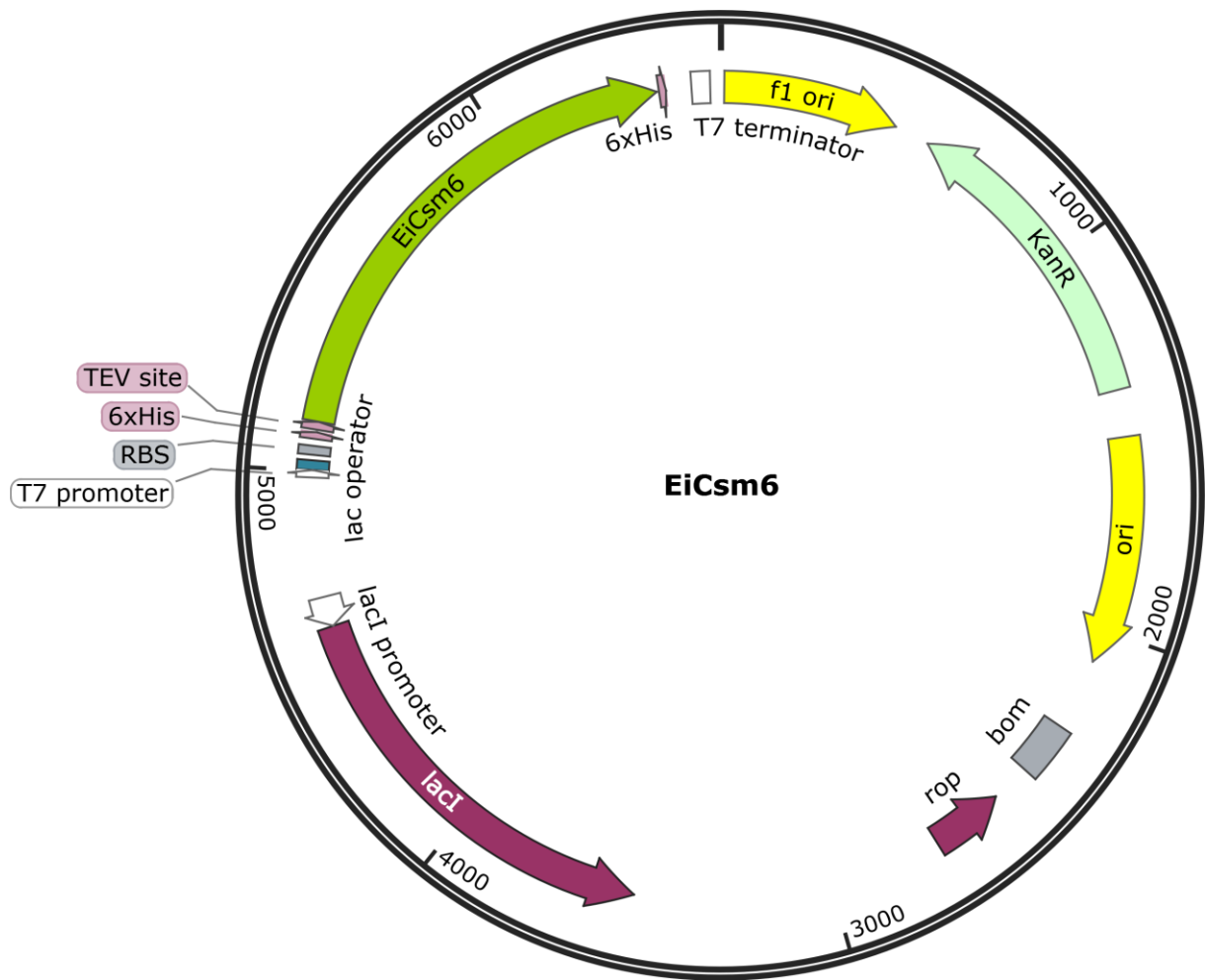


**Figure S2.** Plasmid vector for expression of EiCsm6.

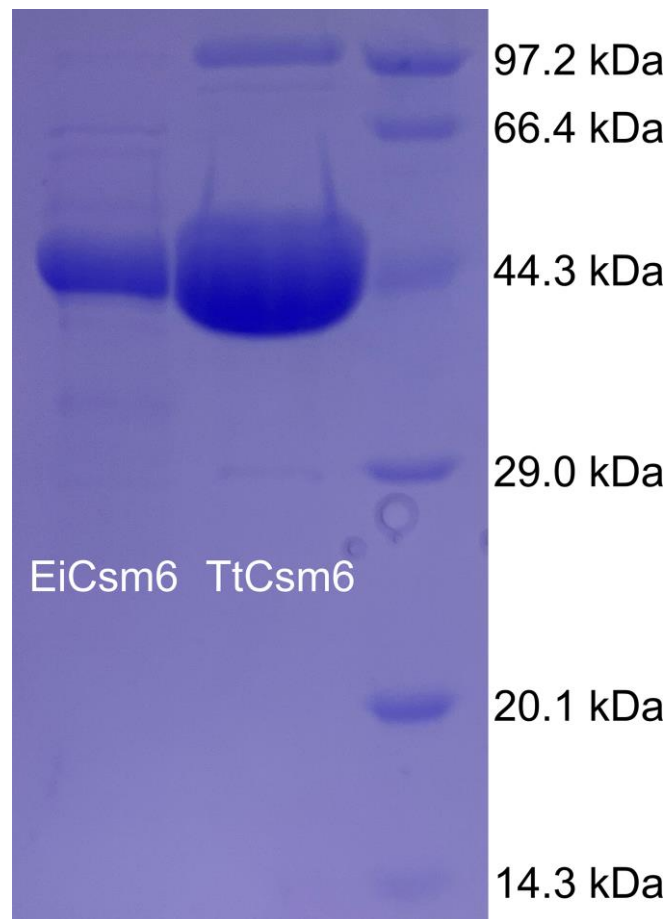


**Figure S3.** SDS-PAGE analysis of purified Csm6 proteins.



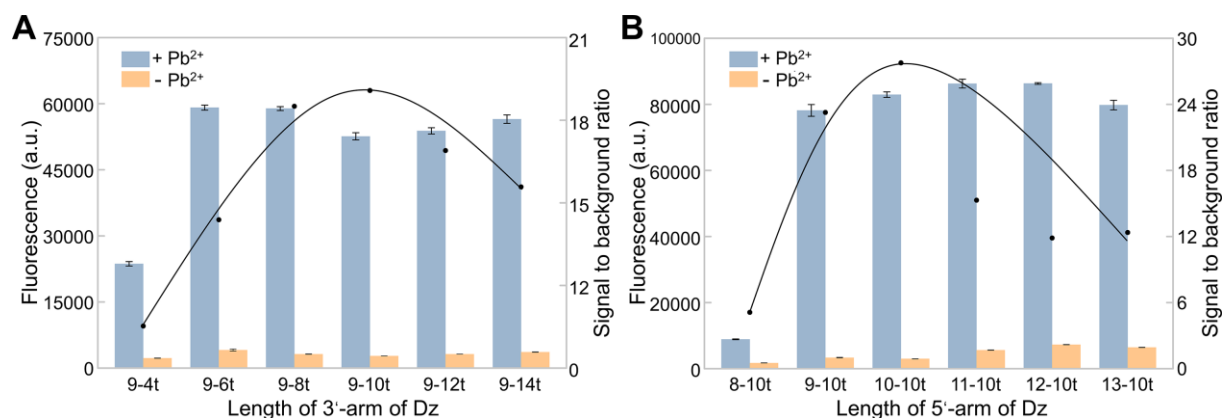


**Figure S4.** Optimization of the lengths of two arms of DNAzyme strand. Fluorescence signal and signal-to-background ratio of the cDNAzyme assay response to Pb<sup>2+</sup> using **Sub** probes that hybridized with **Dz** with different arm lengths (3'-part) (A), different arm lengths (5'-part) (B). The excitation wavelength was 480 nm, with the corresponding emission wavelength of 510-600 nm. The concentrations of Pb<sup>2+</sup>, **Sub** and **Dz** were 150 nM, 400 nM and 400, respectively.

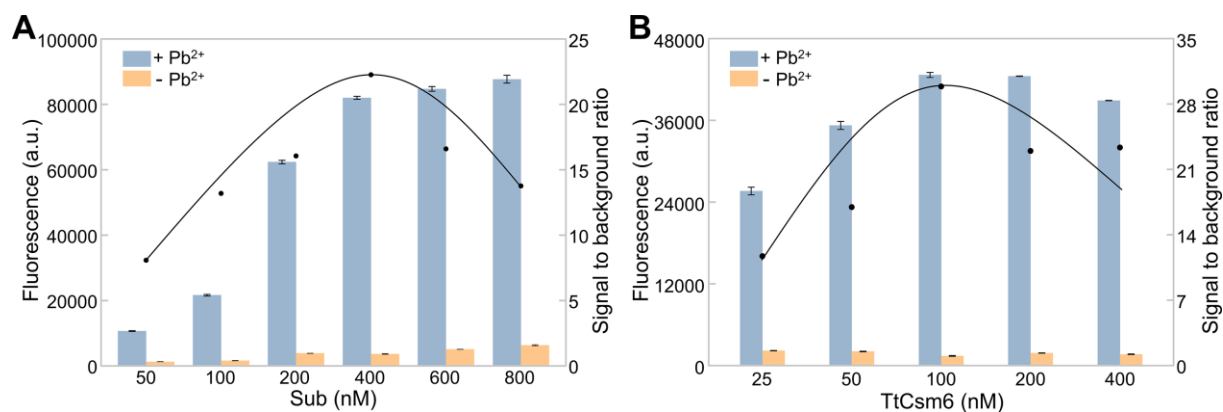


**Figure S5.** Optimization of the concentration of substrate and TtCsm6. Fluorescence signal and signal-to-background ratio of the cDNAzyme assay response to Pb<sup>2+</sup> using different concentrations of **Sub** (A), using different concentration of TtCsm6 (B). The excitation wavelength was 480 nm, with the corresponding emission wavelength of 510-600 nm. The concentrations of Pb<sup>2+</sup>, **Sub** and **Dz** were 150 nM, 400 nM and 400, respectively.

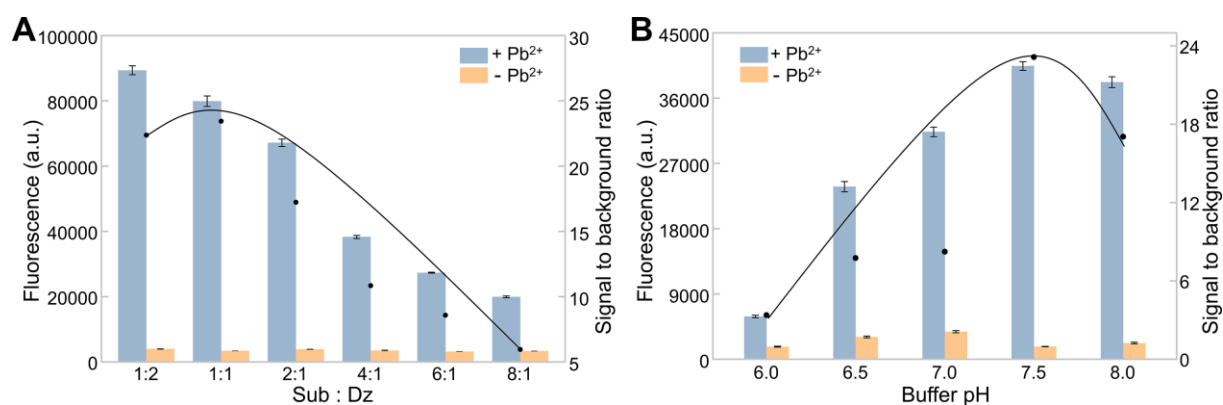


**Figure S6.** Optimization of the amount of DNAzyme strand and buffer pH. Fluorescence signal and signal-to-background ratio of the cDNAzyme assay response to Pb<sup>2+</sup> using different ratios of **Sub** to **Dz** (A), using different buffer pH (B). The excitation wavelength was 480 nm, with the corresponding emission wavelength of 510-600 nm. The concentrations of Pb<sup>2+</sup>, **Sub** and **Dz** were 150 nM, 400 nM and 400, respectively.

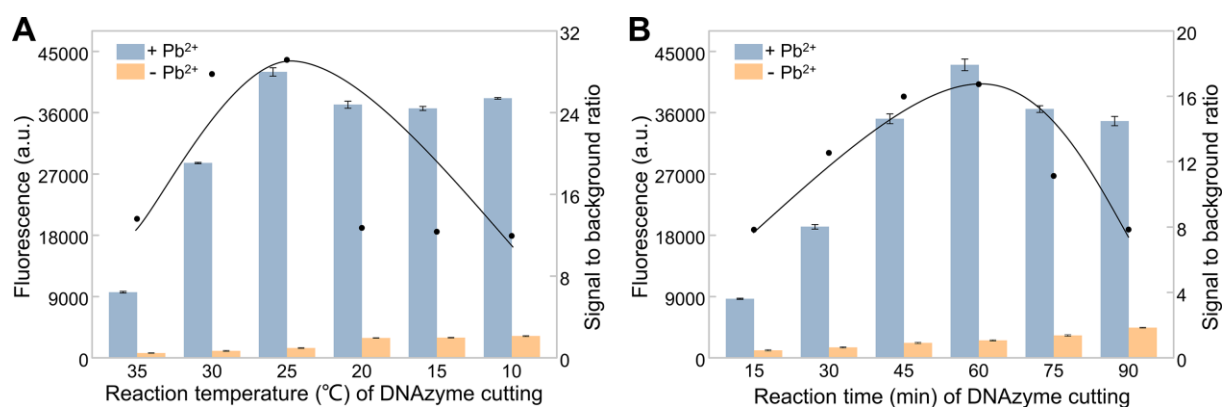


**Figure S7.** Optimization of the reaction temperature and time of DNAzyme cutting.

Fluorescence signal and signal-to-background ratio of the cDNAzyme assay response to Pb<sup>2+</sup> using different reaction temperature (A) and time (B) of DNAzyme cutting. The excitation wavelength was 480 nm, with the corresponding emission wavelength of 510-600 nm. The concentrations of Pb<sup>2+</sup>, **Sub** and **Dz** were 150 nM, 400 nM and 400, respectively.

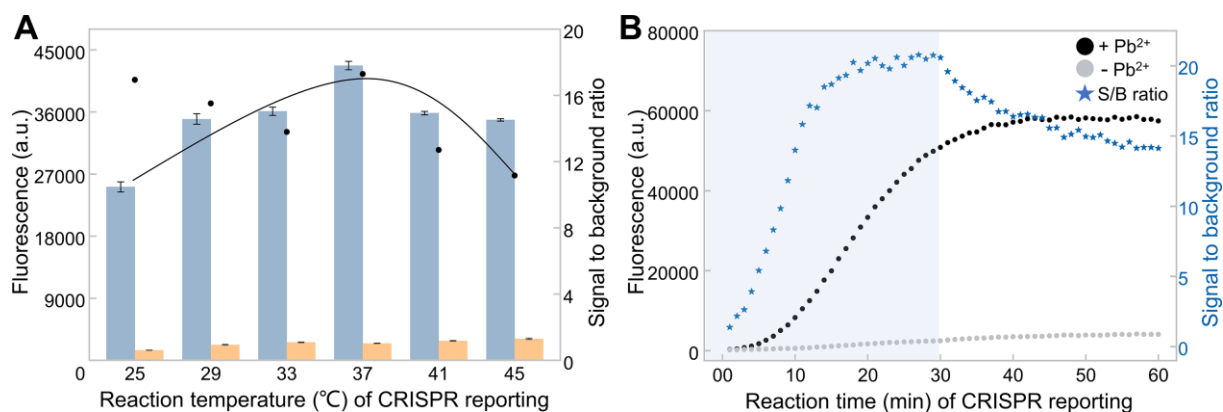


**Figure S8.** Optimization of the reaction temperature and time of CRISPR reporting.

Fluorescence signal and signal-to-background ratio of the cDNAzyme assay response to Pb<sup>2+</sup> using different reaction temperature (A) and time (B) of CRISPR reporting. The excitation wavelength was 480 nm, with the corresponding emission wavelength of 510-600 nm. The concentrations of Pb<sup>2+</sup>, **Sub** and **Dz** were 150 nM, 400 nM and 400, respectively.

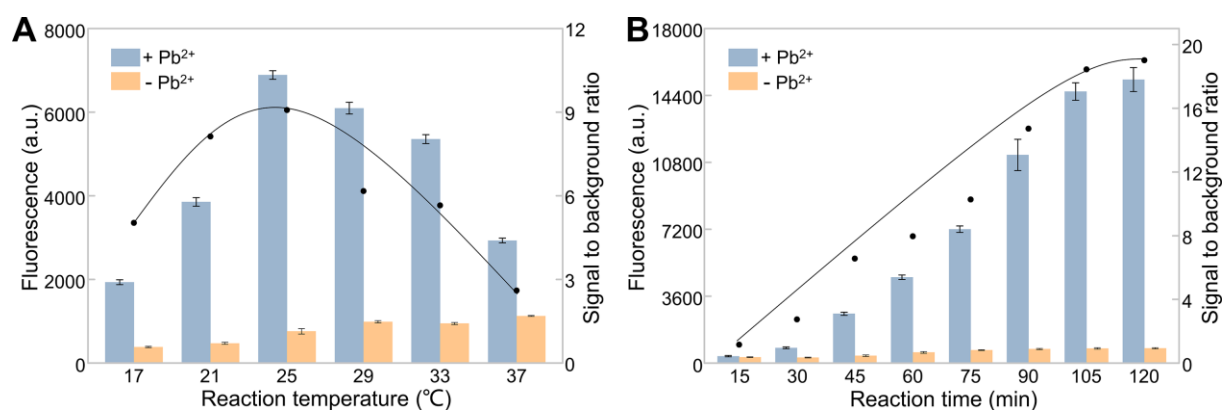


**Figure S9.** Optimization of the one-step cDNAzyme assay for Pb<sup>2+</sup> detection.

Fluorescence signal and signal-to-background ratio of the cDNAzyme assay response to Pb<sup>2+</sup> using different reaction temperature (A) and reaction time (B). The excitation wavelength was 480 nm, with the corresponding emission wavelength of 510-600 nm. The concentrations of Pb<sup>2+</sup>, **Sub** and **Dz** were 150 nM, 400 nM and 400, respectively. The reaction time was 1 h.